

Resonant behavior of the wake of a flat plate: Hot wire and sound scattering measurements

R. H. Hernández¹, M. Vial¹, L. Bellon¹ and C. Baudet²

¹*LEAF-NL, Depto. Ingeniería Mecánica - Universidad de Chile*
Casilla 2777, Santiago, Chile.

²*LEGI, Université Joseph Fourier de Grenoble (UMR 5519)*
1025 rue de la Piscine, BP 53 F-38041, Grenoble cedex 9, France.

abstract

We report experimental measurements of the wake behavior of a thin flat plate submitted to an external harmonic forcing. Two slightly different configurations are examined. Classical hot wire measurements of the velocity field downstream the plate and sound scattering experiments of the near wake demonstrates that the flat plate wake displays a kind of inertial resonance when the inverse of the forcing frequency matches the flying time of fluid particles along the moving part of the plate.

Introduction

Wakes flows from bluff bodies [1], are normally understood as spatially developing open flows, because fluid particles enter and leave the flow boundaries of the observation domain continuously. The particular case of the wake, created by the presence of a thin flat plate, fall into the class of noise amplifiers [2, 3]. This system is very sensitive to external noise, which can, in some situations, be amplified. As every portion of the wake is of convective character (stable or unstable); the system displays, what we call an extrinsic dynamics. That means that the spatial evolution of the flow is essentially determined, either by the external noise entering the system or by a coherent external forcing. The opposite situation is a wake displaying an intrinsic dynamics, either by some adequate hydrodynamic resonance or by the onset of localized regions of absolute instability [4, 5]. The onset of flow structures in this case, become insensitive to the incoming external noise and display a very definite oscillation frequency. Even though, in both cases, the wake's most important signature is the vorticity content [6].

The simplest wake flow is the wake created by a thin flat plate interacting with an uniform laminar flow stream. A real flat plate, of thickness e and length L , does not, in principle, present spontaneous self-sustained oscillations, provided that the Reynolds number based on e , Re_e , be small ($Re_e = U_\infty e/\underline{\nu}$, where $U_\infty, \underline{\nu}$ are the free stream velocity and the kinematic fluid viscosity). In that case the the wake flow acts as noise amplifier. Here,

any initial disturbance externally imposed, is ultimately advected by the mean flow. This sensitiveness to coherent external forcing makes possible to create a very rich family of spatially evolving vortical structures. The onset of dynamical vortical structures at large and small scales will determine any further behavior of the wake.

Wake dynamics characterization, like mean and fluctuating velocity profiles, are normally performed using local measurements of flow velocity (thermal and Laser Doppler anemometry) and recently non-local ones, like PIV methods. However, vorticity, a non local quantity and the most significant ingredient of wake flows, should be measured through non local methods. Scattering of sound waves of high frequency in air (and water) by laminar and turbulent vortex flows has been recently proposed as an accurate diagnosis of such a flows [7, 8, 11, 12, 13].

In vortex flows submitted to sound waves, acoustic scattering occurs as a result of a non linear coupling between flow vorticity and sound. In the first Born approximation, the sound scattered pressure (or density) is found to be proportional to the Fourier transform in space and time of the vorticity of the base flow $\Omega(\mathbf{k}, \nu)$, which constitutes a spectral probe of the vortex flow structure. That linear theoretical relationship is consider to be valid if the incident plane sound wave velocity $\mathbf{v}_i(\mathbf{r}, t)$ and the vortex flow velocity $|\mathbf{u}_v(\mathbf{r}, t)|$ are both small in comparison to the sound velocity c , i.e., $|\mathbf{v}_i| \ll |\mathbf{u}| \ll c$.

If the vortex flow is a slowly varying one, its characteristic time scale T is much longer than that of the sound waves ω the vortex flow appears as frozen by the sound field when $T \gg \omega^{-1}$. Within the first Born approximation, the asymptotic behavior of the scattered pressure field p_s in three dimensions and in the far field region, $\omega|\mathbf{r}|/c \gg 1$, $|\mathbf{r}|/L \gg 1$, is given by the following equation [8],

$$p_s = p_o \frac{i\nu\pi^2}{c^2|\mathbf{r}|} e^{i2\pi\nu\mathbf{r}/c} \frac{\cos\theta}{1 - \cos\theta} \tilde{\Omega}_z(\mathbf{q}, \nu - \nu_o) \quad (1)$$

where we see that $\tilde{\Omega}(\mathbf{q}, \nu - \nu_o)$ corresponds to the Fourier transform in space and time of the base flow vorticity $\Omega(\mathbf{r}, t) = \nabla \times \mathbf{U}(\mathbf{r}, t)$. The scattering wave vector, as in light scattering theory, is given by $\mathbf{q} = \mathbf{k}_d - \mathbf{k}_i$ for $\nu \sim \nu_o$. If r is the distance between the vortex target and measuring point, to look for asymptotic plane scattering waves we have to consider the two conditions $r/\lambda \gg 1, r/L \gg 1$, of the far field approximation.

From an experimental point of view, a flow diagnostic is possible if we can get an overall representation, in Fourier space, of a wide range of scattering wave vectors \mathbf{q} . If we consider a symmetric geometrical representation of the incident and scattered wave vectors, the scattering wave vector can be approximated (according to a particular choice of a reference frame) by

$$\mathbf{q} = \frac{4\pi\nu_o}{c} \sin(\theta/2)\hat{x} \quad \text{with} \quad \mathbf{q} \cdot \hat{y} = 0$$

In that form, a flow diagnostic can be done by two ways; changing the scattering angle θ or varying the incoming sound frequency ν_o . The second way is easy to achieve, because a simple frequency sweep provides an overall response at all wave vectors. Scattering signals in the above theoretical form are pressure signals. They must be measured by accurate pressure transducers of both high sensitivity and specially high spatial resolution. Spatial resolution is ultimately limited by diffraction effects due to transducer's size. The incoming sound waves involved in theoretical calculations are plane waves, and that can be provided, for instance, by a flat and large emitter. However the receiver can be either a

large transducer or a small one. The large one enables the right definition of the scattered wave vector, thus allowing to probe the flow at different scales. A small one should be used to trace the interference pattern coming from a multitude of scattered wave vectors. This paper is concerned with the pattern forming structures on the wake of a flat plate under external forcing. Results from two experiments are shown on the basis of classical hot wire measurements of the near wake and through the scattering of sound waves by flow vorticity of the wake.

Experimental set-up

Two flat plates models are investigated. The first case (hereafter case **I**) considers a thin and rigid flat plate (copper, small roughness) of aspect ratio length-to-thickness $L/e = 25$, with thickness $e = 1.6$ mm. The plate maintained in vertical position, can perform small oscillations, through two half-axes passing at the geometric center of the front end of the plate (border of attack). We use ball-bearings supporting axes to perform oscillatory forcing reducing friction. (Fig. 1 a).

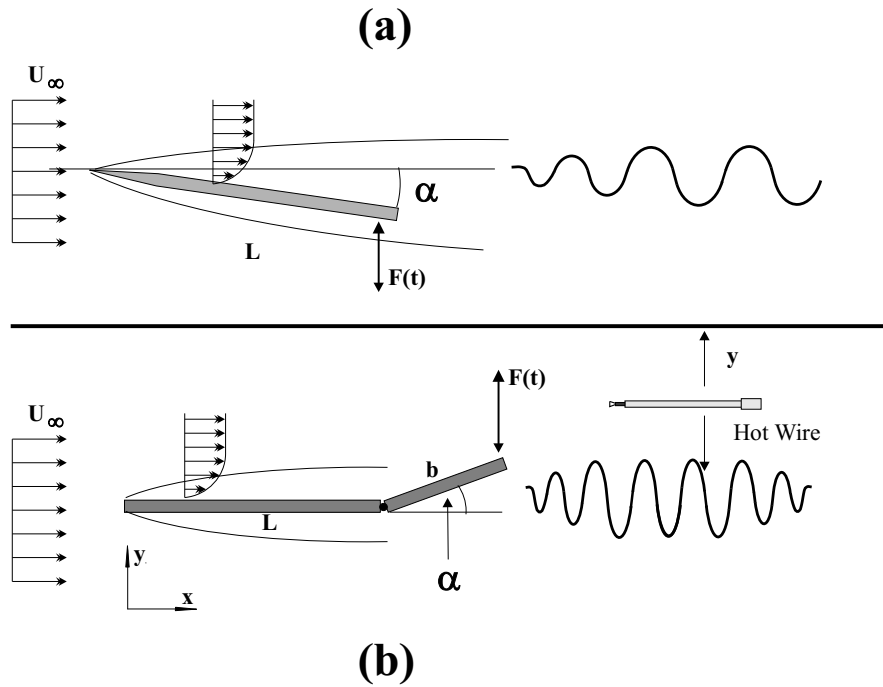


Figure 1: *Physical set up. (a) Case I. A rigid flat plate of length L and width e , oscillating at small angles α around the border of attack. (b) Case II. A fixed flat plate of length L , with a short flap b at the trailing edge, performing small oscillations. For both systems, incoming fluid flow was a flat velocity profile (below 1 %) of controlled free stream velocity U_∞ .*

The second thin plate system (hereafter case **II**) consist of a fixed flat plate of length L with a small flap of length b at the trailing edge (supported by small ball-bearings), which can perform small oscillations when forced by an external shaker. The aspect ratios are: length-to-thickness $L/e = 12.5$, flap length-to-thickness $b/e = 18.7$ (Fig. 1 b). The first model was tested in the open low turbulence wind tunnel at the Physics laboratory (Ecole

Normale Supérieure-Lyon). This wind tunnel reaches a maximum free stream velocity of $U_\infty = 2$ m/s, with a rate of turbulence less than 0.05 %.

The second model was tested in the closed (double section) wind tunnel at the LEAF-NL laboratory, (Universidad de Chile). For this tunnel, the maximum free stream velocity is $U_\infty = 20$ m/s with a turbulence rate less than 0.5 %. Leading and trailing edges for both flat plate models are similar.

Harmonic forcing, in both cases, was performed with a B&K 4810 electromagnetic shaker coupled to a rigid aluminum arm system attached to: both sides of the plate for the first case, and to the both sides of the flap, in second case. Both systems were mounted on a completely independent support, uncoupled from the wind tunnel in order to avoid undesired vibrations from fans. Measurements of wake velocity profiles were made with hot wire probes at different downstream distances (x/e coordinate) from the plate's trailing edge.

Hot wire Results

The free regime without forcing (Fig.2) as well as the accurate wake response to different forcing regimes (Fig.3), was obtained by systematic measurements of the whole wake velocity profiles using thermal anemometry. Scanning the cross stream coordinate (y/e) across the wake with the hot wire probe coupled to a stepper motion provides a clear but complementary picture of the wake dynamics (velocity profiles) before to proceed with scattering experiments.

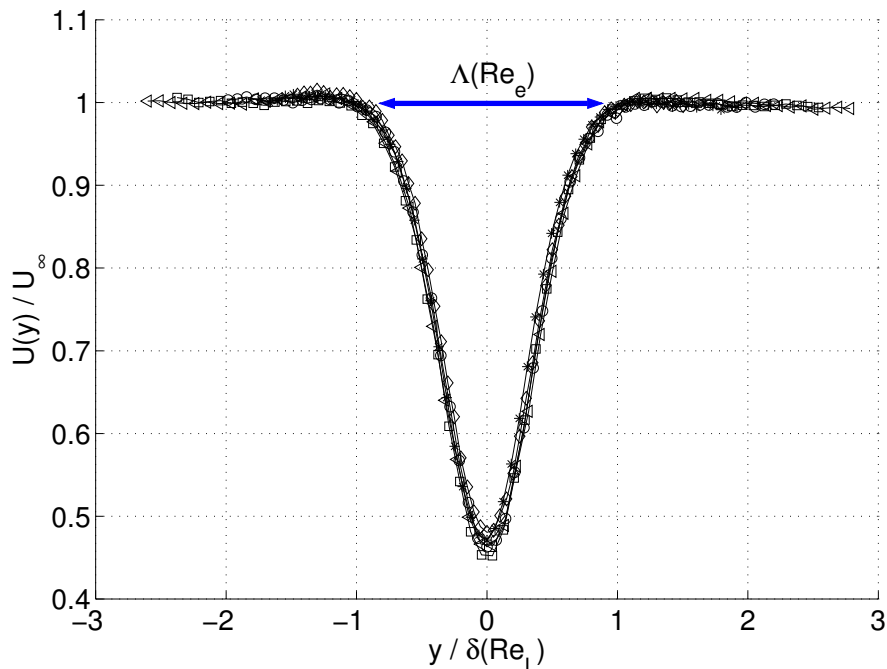


Figure 2: Case II: Normalized velocity profiles $U(y)/U_\infty$ when the flap is in horizontal position (without forcing), for $x/e = 31.2$, $\alpha = 0$, at different values of the width based, e , Reynolds number Re_e : \diamond , 54,6; $*$, 83,2; \circ , 109,3; \square , 151,2; \triangleleft , 181,2.

Without forcing

In cases **I** and **II**, we recorded mean velocity profiles $U(y)$ as a function of Reynolds number Re_e . In both situations, velocity profiles are symmetric with respect to $y/e = 0$, where the minimum wake velocity (at any x/e position) is found. Wake width and Reynolds number are related through the effects on the upstream boundary layer (on the plate).

We found that the greater the Re_e the thinner the wake. However, all normalized velocity profiles (by U_∞) collapse into a single curve when we scale the transverse coordinate with the estimated boundary layer thickness at the trailing edge of the plate $\delta(Re_L)$, as we see in Fig. 2. The wake thickness is of the order of $\sim 2\delta(Re_L)$ at any of the Reynolds values.

Harmonic forcing

The forcing mechanism is exactly the same in both situations. When the flap (Case **I**) or the overall plate (Case **II**) are forced to oscillate harmonically at small angles α , the natural wake is modulated at the forcing frequency f_0 . The angle is given by

$$\alpha(t) = \alpha_m \sin(2\pi f_0 t) \quad (2)$$

where α_m the maximum forcing angle and f_0 the forcing frequency, and we define $\alpha_{pp} = 2\alpha_m$ as the peak-to-peak value.

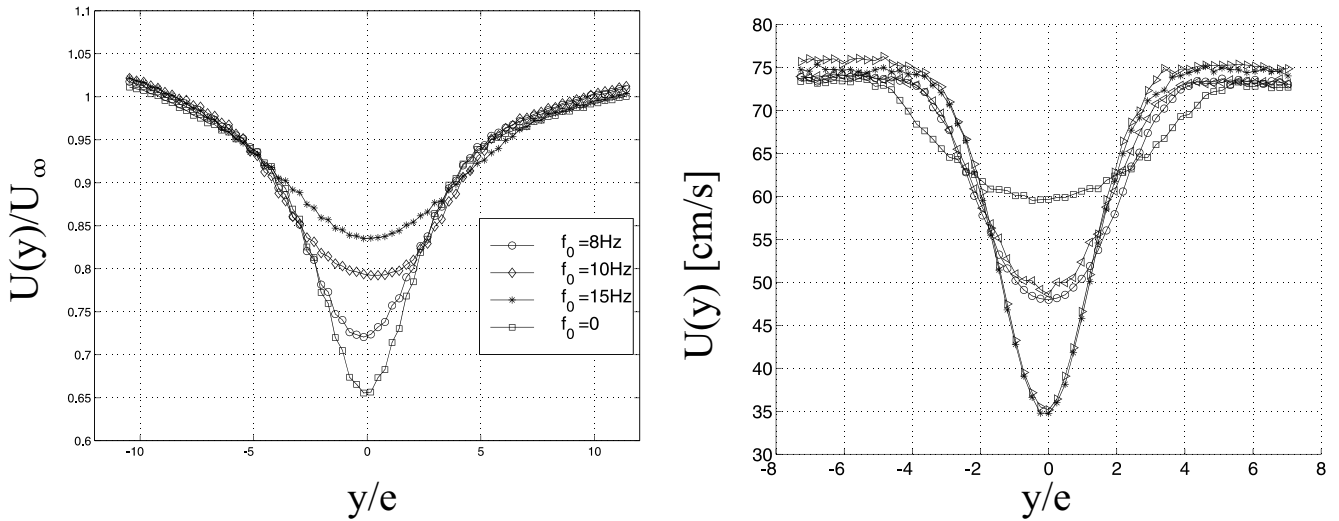


Figure 3: Case **I**: Systematic effect of forcing frequency on the wake behavior ($x/e = 79.4$) at constant but small peak-to-peak amplitude of the order of $2b\alpha_m/e \sim 0.2$ and Reynolds number $Re_b = 47.4$. (a) Mean velocity profiles $U(y)/U_\infty$. Free wake behavior is indicated by a \square ($f_m = 0$ Hz). Case **II**: Mean velocity profiles $U(y)$ for different forcing frequencies f_0 : $*$, 1 [Hz]; o , 18 [Hz]; \square , 25 [Hz]; \triangleleft , 33 [Hz]; \triangleright 44 [Hz]. Reynolds number is $Re_e = 83.2$ and $x/e = 31.2$

A significant difference between the free and forced wake is the cross stream increased scale of the later. The effect of harmonic forcing, for the Reynolds numbers here studied, is to increase the wake width, defined as $\Lambda(Re_e)$, with respect to the free case. However, the wake width will depend on f_0 provided that the peak-to-peak forcing amplitude be constant. In any case, the wake displays an oscillatory and periodic motion at the forcing frequency f_0 which consist of spatial vorticity waves advected at an average velocity downstream the

flat plate. A simple estimation for the wave length of the spatial vorticity pattern, λ_Ω , can be the ratio between the free stream mean velocity and the forcing frequency, $\lambda_\Omega \sim U_a/f_0$. This spatially periodic pattern can be understood if we consider the spatial and temporal Fourier transform of the vorticity equation in 2D, (neglecting diffusion terms). A dispersion relation relating frequency f and wave number \mathbf{k} , of the form; $2\pi f = \mathbf{k} \cdot \mathbf{U}_a$ where $\mathbf{U}_a \cdot \hat{x}$ is the advection velocity of vorticity and $|\mathbf{k}| = 2\pi/\lambda_\Omega$.

This relationship will explain a Doppler effect associated to scattered pressure signals [12]. We will prove that sound scattering will be intense when the scattering wave vector q matches the wave length of the spatial vorticity pattern λ_Ω .

The wake width difference that is seen between overall velocity profiles from case **I** and **II** under forcing (Fig. 3) can be explained because hot wire measurements in case **I** were made at higher x/e distances from the trailing edge and the wake width increases with longitudinal coordinate x . At similar measuring points, both wakes under similar forcing parameters, α, f_0 , are similar.

A simple dimensionless analysis of the general situation gives us three characteristic time scales, t_L, t_b, t_0 , defined as follows.

$$t_L = \frac{L}{U_\infty} \quad t_b = \frac{b}{U_\infty} \quad t_0 = \frac{1}{f_0} \quad (3)$$

Both times scales, t_L and t_b are equivalent, and correspond to the flying time required for fluid particles to move along that length scale of the plate which is under forcing. In case **I** it is the whole plate L which performs oscillations, and in case **II** it is only the small flap b . The last time scale t_0 is simply the inverse of the forcing frequency.

The two dimensionless parameters involving those time scales are the ratios $F_b = t_b/t_0$ and $F_L = t_L/t_0$ which are understood as the inertial response of the flow around the boundary layer to a periodic forcing. If we increase f_0 enough such that $F \gg 1$, fluid particles inside the boundary layer are now submitted to a harmonic forcing in time, and we can now trigger instabilities of the boundary layer itself [15].

For the particular condition $F_b, F_L \sim n$ where $n = 1, 2, 3, \dots$, the system will display some kind of inertial resonance, as the flying time equals the forcing period, and fluid particles of each plate side, leave the trailing edge at zero angle $\alpha = 0$. This behavior is seen in Fig 3, where mean velocity profiles (case **II**) are wider when F_b approaches unity (or f_0 is 25 Hz).

To find out the wake response to systematic forcing from wake velocity measurements, we look for energy, or velocity fluctuations, profiles downstream the system. Fig. 4 displays the wake frequency response in the form of integrated mean squared values of velocity fluctuations $\langle u^2 \rangle$ as a function of forcing frequency f_0 , for three different Reynolds values. In any case, energy fluctuations are maximum at three resonant forcing frequencies $f_r \sim 15, 25, 29$ Hz, for Reynolds numbers of $Re_e = 59, 104, 83$ respectively. Note that in these experiments, the averaged forcing energy, is very small, $\langle E_f \rangle \propto \alpha_m^2 f_0^2$ represents around 3% of kinematic flow energy. This resonant behavior is obtained if the dimensionless parameter F_L, F_b are close to unity. In this case, the wake pattern adopts the form of periodic modulated vorticity sheets of wavelength $\lambda_\Omega \sim U_\infty/f_r$ where f_r corresponds to the resonant forcing frequency. The resonant behavior, in the form of maxima of integrated fluctuating energy, must be related to the vorticity of the wake. The following scattering experiments, will provide a proof of this inertial resonance.

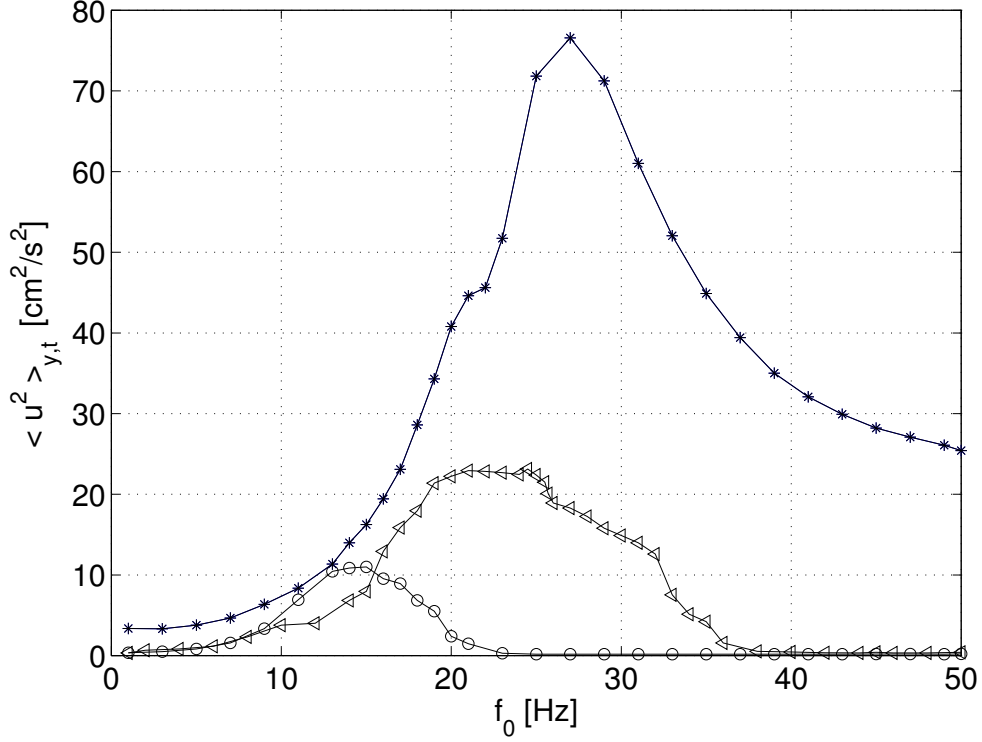


Figure 4: Case II: Integrated mean squared energy fluctuations $\langle u^2 \rangle$ versus forcing frequency f_0 , at three Reynolds numbers Re_e : \circ 59; \triangleleft 83; $*$ 104. Resonance frequencies are $f_r \sim 15, 25, 29$ Hz respectively.

Sound scattering

As mentioned before, sound scattered pressure p_s is proportional to the spatio-temporal Fourier transform of vorticity, $\Omega(\mathbf{q}, \nu)$. According to our experimental conditions for case I, the scattering wave vector, defined as $\mathbf{q} = \mathbf{k}_s - \mathbf{k}_i$, can be written as $q \sim 4\pi(\nu_o/c) \sin(\theta/2)\hat{x}$ because $\mathbf{q} \cdot \hat{y} = 0$ in Fig 5.

Experiments were performed as in Fig 5, looking for a symmetrical configuration. Both the sound emitter and receiver are square Sell type transducers of size $\Lambda = 15$ cm, having a flat response between 5 to 100 kHz within 10 dB. Details can be found in [11, 12].

The emitter and receiver (placed outside the test section) are focused toward the near wake of the plate (Fig. 5). The incident, \mathbf{k}_i , and scattered, \mathbf{k}_s , wave vectors forming an angle θ . With such a geometry we probe the vortex flow at length scales corresponding to the wave vector $\mathbf{q} = \mathbf{k}_s - \mathbf{k}_i$ of components $q_y = 0$ and $q_x = 4\pi(\nu_o/c) \sin(\theta/2)$. At constant scattering angle $\theta = 30^\circ$, different wave vectors \mathbf{q} are obtained by simply setting the emitter frequency ν_o .

A heterodyne detection procedure (demodulation of the received acoustic signal) gives us an analytic signal [16] that can be sampled at low-frequency. The phase of this analytic signal is directly related to the Doppler shift and the amplitude proportional to vorticity content of the periodic flow inside the scattering volume.

As we have shown above, harmonic forcing on the flat plate, traduces into an oscillatory wake pattern. Any wake modulation traduces into a vorticity modulation at the forcing frequency f_0 . The fact that the scattering pressure signal, p_s , displays a Doppler frequency

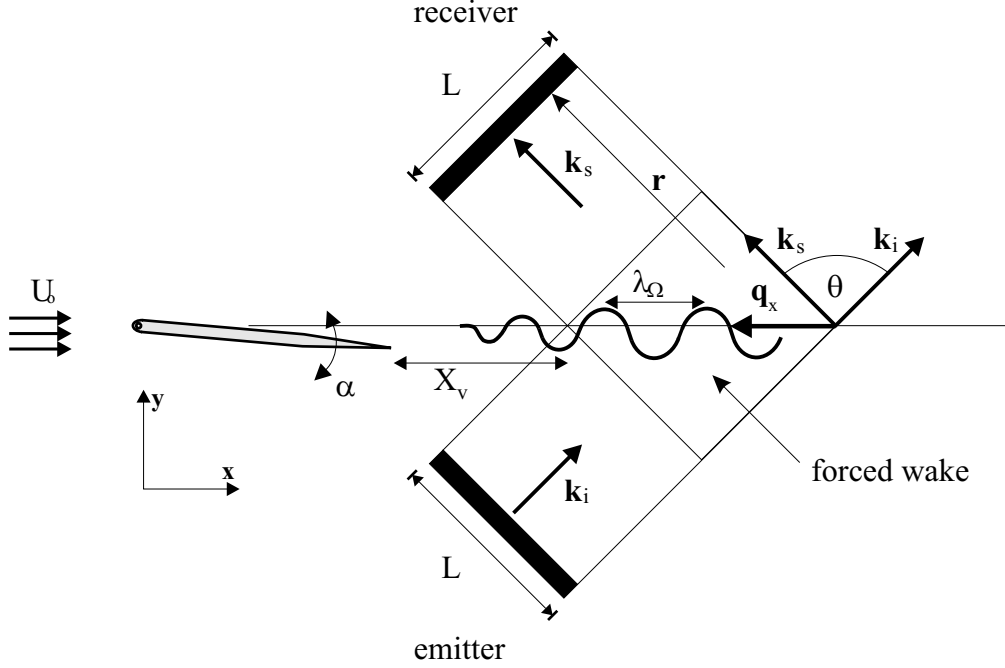
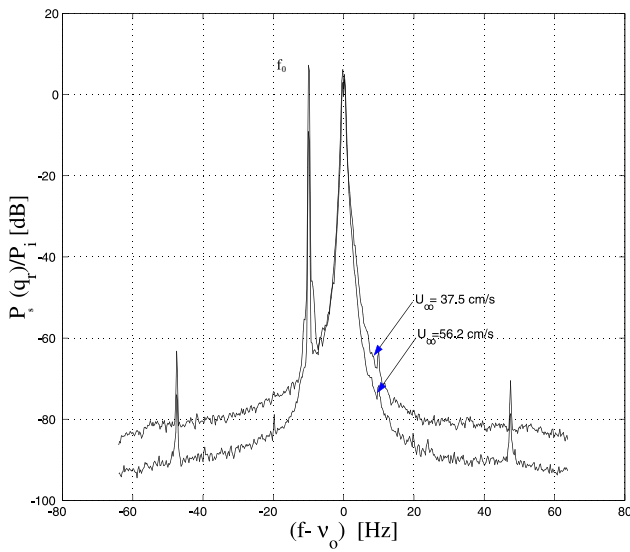


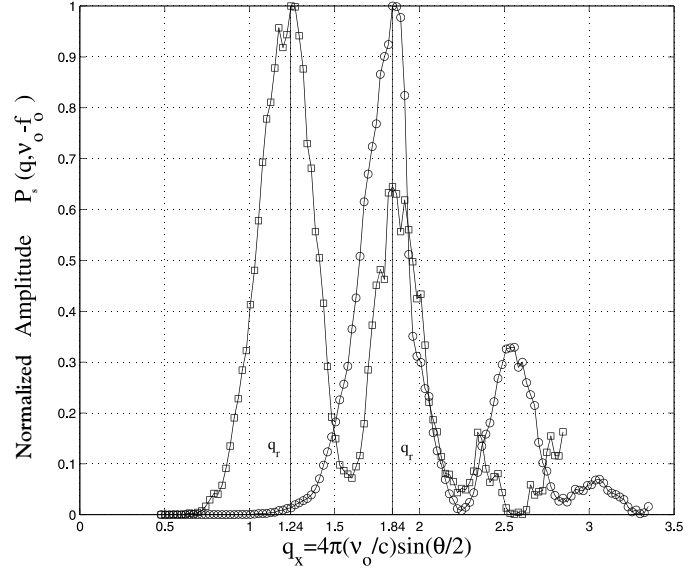
Figure 5: *Sound scattering experimental set up. Square (size $\Lambda = 15$ cm) Sell type ultrasound emitter and receiver under a symmetric configuration. The scattering angle between the incident (k_i) and the scattered (k_s) wave vector is $\theta = 30^\circ$. The beginning of the scattering volume, x_v , corresponds to a $x_v/b = 13$ ratio downstream the plate.*

shift ($\Delta\nu = f_0 - \nu_0$), where its sign is given by the sense of the scattering wave vector q originates because the vortex target is moving at an advection velocity close to the mean free stream flow velocity. After a heterodyne demodulation, the power spectrum of the scattered pressure signal is centered at ν_0 and one measures with good accuracy ($d\nu = 50$ mHz) the spectral line associated to the scattered pressure p_s , as shown in Fig. 6 (a). The scattering peak occurs exactly at $\Delta\nu = -f_0$, independent of the advection velocity, in agreement with theory. An overall wave scattering vector scanning, provides the peak amplitude at the forcing frequency from each of the power spectra of scattered pressure. Fig. 6 (b) displays two clear resonances of the power spectrum amplitude as a function of the scattering wave vector q . However, two different flow velocities are involved. This is explained only if we respect the dispersion relationship stated in the previous section. Forcing frequency, scattering wave number and flow velocity obey $2\pi f = \mathbf{q} \cdot \mathbf{U}_a$ where $\mathbf{U}_a \cdot \hat{x}$ is the advection velocity of vorticity ($U_a \sim U_\infty$) and $|\mathbf{q}| = 2\pi/\lambda_\Omega$. The Doppler shift is invariant, and if we take the resonant wave vectors of Fig 6, with their associated velocities, the dispersion relationship is exactly fulfilled. An estimate of U_a is given by the averaged flow velocity inside the wake.

If we trace the power spectrum amplitude at the Doppler peak for resonant wave vectors (constant Reynolds, Re_e), we get an overall vorticity resonance as shown in Fig. 7. The resonance occurs when the dimensionless parameter, in this case F_L , is close to unity. When $F_L \sim 1$, the wavelength of the periodic vortex motion inside the wake, λ_Ω is an exact multiple of the flat plate length scale L , and, as we stated before, the wake width is maximum, so we conclude that vorticity resonance are directly related to the wake's transverse extension.



(a)



(b)

Figure 6: Ultrasound scattering by the forced wake at two different free stream velocities $Re_e = 40$ (\square), $Re_e = 60$ (\circ), where the forcing amplitude and frequency are : $2L\alpha_m/e \sim 0.2$, and $f_0 = 10$ Hz, respectively. (a) The power spectra of scattered pressure display the same Doppler peak at the forcing frequency f_0 . (b) A sweep of the scattering wave vector $q = 4\pi(v_0/c)\sin(\theta/2)$ indicate two clearly different spatial resonances at very definite length scales (q_r).

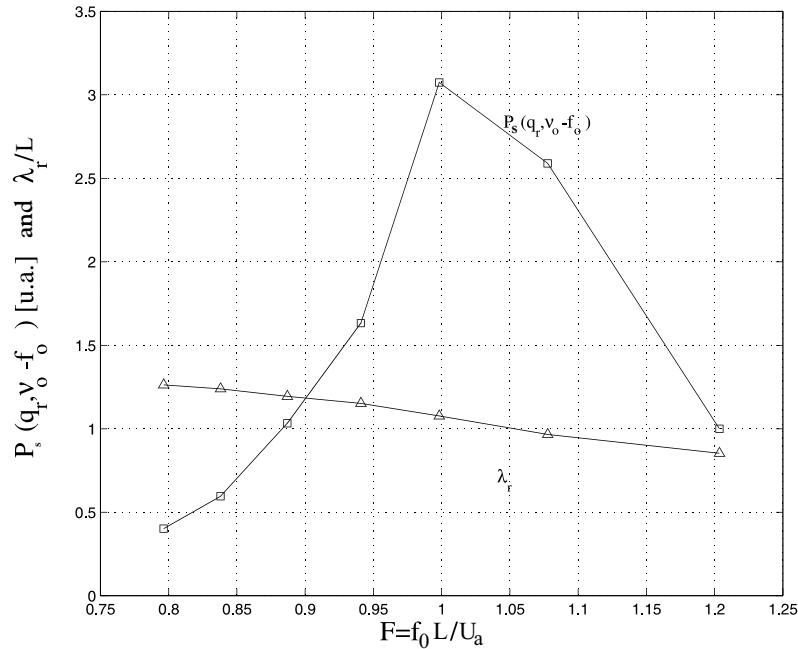


Figure 7: Evolution of the normalized resonant scattered pressure amplitudes (\square) and resonant wavelengths (\triangle) with the dimensionless parameter $F_L = f_0 L / U_a$.

Concluding remarks

A complete investigation of the wake resonant behavior, in two slightly different situations (case **I**, **II**), was accomplished using both classical hot wire anemometry and ultrasound scattering methods. The aim of this experimental work was to study and compare the dynamical response of the laminar wake of a flat plate under two slightly different forcing methods. In a first case, forcing was introduced by small amplitude rotary oscillations of the trailing edge of a flat plate. In a second case, the flat plate was composed of a static part plus a small flap attached to the trailing edge, that was in oscillatory forced motion. Both methods confirmed the presence of a resonant wake behavior. At the resonance condition, the wake width is maximum, and vorticity displays a maximum amplitude. In addition, sound scattering results, confirm that Doppler effect is in agreement with recent theoretical findings, in particular that the Doppler shift and wave length of vorticity obey accurately the scalar product $\mathbf{q} \cdot \mathbf{U}$.

Acknowledgments

Grants Fundación Andes C-13600/4, Fondecyt N° 1990571 and Fondecyt N° 3010067 are gratefully acknowledged.

References

- [1] M. Schumm, E. Berger and P. A. Monkewitz, Self-excited oscillations in the wake of two-dimensional bluff bodies and their control, *J.Fluid Mech.*, **271**, pp.17, 1994.
- [2] A. Couairon and J. M. Chomaz, Global instability in fully nonlinear systems, *Phys.Rev.Lett*, **77**, pp. 4015, 1996.
- [3] P. Huerrre, Local and Global Instabilities in Spatially Developing Flows. *Annu. Rev. Fluid Mech.*, **22**, pp.473, 1990.
- [4] M. Provansal, C. Mathis and L. Boyer, Bénard-von Kármán instability: transient and forced regimes, *J.Fluid Mech.*, **182**, pp. 1, 1987.
- [5] R. H. Hernández and C. Baudet, A new perturbation method. Application to the Bénard-von Kármán instability, *Europhys. Lett.*, **49** (3), pp. 329, 2000.
- [6] R. H. Hernández and C. Baudet, Ultrasound Scattering by Forced Laminar Wakes. *Lecture Notes in Physics, Vortex Structure and Dynamics*, A. Maurel and P. Petitjeans (eds.), Springer Verlag, 2000.
- [7] A. L. Fabrikant, Sound scattering by vortex flows, *Sov.Phys.Acoust.*, **29**, (2), pp. 152, 1983.
- [8] F. Lund and C. Rojas, Ultrasound as a probe of turbulence, *Physica D*, **37**, pp. 508, 1989.
- [9] M. Gharib and K. Williams-Stuber, Experiments on the Forced Wake of an Airfoil. *J. Fluid Mech.* **208**, pp. 225, 1989.

- [10] J.J. Miao, C. R. Chen and J. H. Chou, A vertically Oscillating Plate Disturbing the Development of a Boundary Layer. *J. Fluid Mech.*, **298**, pp. 1, 1995.
- [11] C. Baudet, S. Ciliberto and J.-F. Pinton, Spectral analysis of the von Kármán flow using ultrasound scattering, *Phys.Rev.Lett.*, **67**, (2), pp. 193, 1991.
- [12] J.-F. Pinton and C. Baudet, Measurements of vorticity using ultrasound scattering, in *Turbulence in spatially extended systems*, Nova Science Publishers, 1993.
- [13] J.-F. Pinton, C. Laroche, S. Fauve and C. Baudet, Ultrasound scattering by buoyancy driven flows, *J.Phys. II France*, **3**, pp. 767, 1993.
- [14] S. Candel, *Mécanique des fluides*, Dunod, Paris, 1990.
- [15] J. J. Healey, A new boundary layer resonance enhanced by wave modulation: theory and experiment, *J. Fluid Mech.*, **304**, pp. 231, 1995.
- [16] A. Papoulis, *Probability, Random Variables and Stochastic Processes*, McGraw Hill, New York, 1965.